Krauskopf, B., & Erzgraber, H. (2008). *Delay-coupled semiconductor lasers near locking: a bifurcation study.* http://hdl.handle.net/1983/1073

Early version, also known as pre-print

Link to publication record on the Bristol Research Portal
PDF-document

Delay-coupled semiconductor lasers near locking: a bifurcation study

Bernd Krauskopf[a] and Hartmut Erzgräber[b]

[a] Department of Engineering Mathematics, University of Bristol,
Bristol BS8 1TR, United Kingdom
[b] School of Engineering, Computing and Mathematics, University of Exeter,
Exeter EX4 4QF, United Kingdom

ABSTRACT

We consider a system of two identical, but possibly detuned, spatially separated semiconductor lasers that are mutually coupled via their optical fields. In a rate equation approach this system can be modeled by a set of delay differential equations, where the delay takes into account the propagation time of the light from one laser to the other. The delay introduces a complicated structure the compound laser modes (CLMs) whose interaction may lead to complicated dynamics.

In this paper we present a bifurcation study of the CLM structure for the relevant system parameters, including the pump current and the detuning. Initially stable CLMs can destabilizes in Hopf bifurcations that lead to complicated dynamics on different time scales. In particular, we concentrate on the dynamics near the boundary of locked dynamics of the two lasers. Depending on the pump current we find different scenarios for the route to locking as a function of the detuning between the two lasers.

Keywords: semiconductor laser, delay-coupling, routes to locking

1. INTRODUCTION

Our object of study is a system consisting of two mutually delay-coupled semiconductor lasers, where the delay arises because of the spatial separation of the coupled sub-systems; see the sketch in Figure 1. From a technological point of view, delay-coupled lasers are of interest because of applications including bistable devices for optical flip-flops, high-frequency generation for optical clocks, and secure communication with a chaotic carrier; see, for example, Refs. [1–3]. From a fundamental point of view, this system is of interest for the study of coupled non-linear optical elements; see, for example, Ref. [4–7]. Of particular interets are issues of locking and synchronization in the presence of delays; see Refs. [5, 8–11].
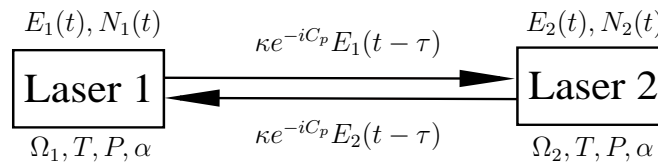
Figure 1. Sketch of the system of two delay-coupled semiconductor lasers.

In this paper the dynamics of laser 1 and laser 2 are modelled by rate equations for the slowly varying envelope of the optical field $E_{1,2}(t)$ and the inversion $N_{1,2}(t)$. In dimensionless form they can be written as:

$$
\begin{aligned}
\dot{E}_1(t) &= (1+i\alpha)N_1(t)E_1(t) + \kappa e^{-iC_p}E_2(t-\tau) - i\Delta E_1(t), & (1)\\
T\dot{N}_1(t) &= J - N_1(t) - (1+2N_1(t))|E_1(t)|^2, & (2)\\
\dot{E}_2(t) &= (1+i\alpha)N_2(t)E_2(t) + \kappa e^{-iC_p}E_1(t-\tau) + i\Delta E_2(t), & (3)\\
T\dot{N}_2(t) &= J - N_2(t) - (1+2N_2(t))|E_2(t)|^2. & (4)
\end{aligned}
$$

1

Table 1. Laser parameters and their values.

laser parameter	value
linewidth enhancement factor	2.0
photon decay rate	150ns^{-1}
differential gain	790ns^{-1}
carrier density at threshold	10^{18}
coupling rate	7ns^{-1}
coupling time	0.17ns
coupling phase	0
detuning	*free*
pump parameter	*free*

Here time t is measured in units of the photon lifetime. A fraction of the light emitted by laser 1 is coupled into laser 2 and vice versa, where κ determines the coupling strength and C_p is the coupling phase. The time delay τ in the coupling terms takes into account the propagation time of the light in the gap of length l between the lasers; hence, $\tau = \frac{l}{c}$ where c is the speed of light. The parameter

$$\Delta = \Omega_2 - \Omega_1 \tag{5}$$

is the detuning between the optical frequencies, Ω_1 and Ω_2, of the two lasers. The remaining parameters are the linewidth enhancement factor α, the normalized carrier lifetime T, and the pump parameter J. We consider here the values $\alpha = 2.0$, $T = 150.0$, $\tau = 25.49$, and $\kappa = 0.047$, which were derived from the physical values in Table 1. Furthermore, throughout this study we consider the case of a fixed feedback phase $C_p = 0$; see Ref. [12] for the influence of this parameter. The parameters that we vary in this study are the detuning Δ and the pump current J.

As for the Lang-Kobayashi rate equations for a laser with conventional optical feedback [13], the main modeling assumptions are that the lasers operate in single mode and that the feedback rate is small enough so that multiple round-trips can be neglected; see Ref. [14] for a detailed derivation of Eqns. (1)–(4).

2. CHARACTERISTIC DYNAMICS NEAR THE LOCKING RANGE

The compound laser modes (CLMs) are the basic solution of the rate equation model Eqns. (1)–(4). They correspond to cw-emission of the coupled laser system and, hence, to locked output of the coupled laser system. The CLMs can be written as:

$$
\begin{aligned}
E_1(t) &= |E_1^s| e^{i\omega^s t}, & (6) \\
E_2(t) &= |E_2^s| e^{i\omega^s t + i\sigma}, & (7) \\
N_1(t) &= N_1^s, & (8) \\
N_2(t) &= N_2^s, & (9)
\end{aligned}
$$

where $|E_{1,2}^s|$, $N_{1,2}^s$, ω^s and σ are real valued. In this ansatz $|E_{1,2}^s|$ are the positive amplitudes of the optical fields and $N_{1,2}^s$ the inversions of laser 1 and 2, respectively. Further, ω^s is the lasers's common optical frequency with respect to the mean frequency $\Omega = (\Omega_1 + \Omega_2)/2$, and σ is a time-independent phase shift; see Ref. [12] for a comprehensive study of the CLMs.
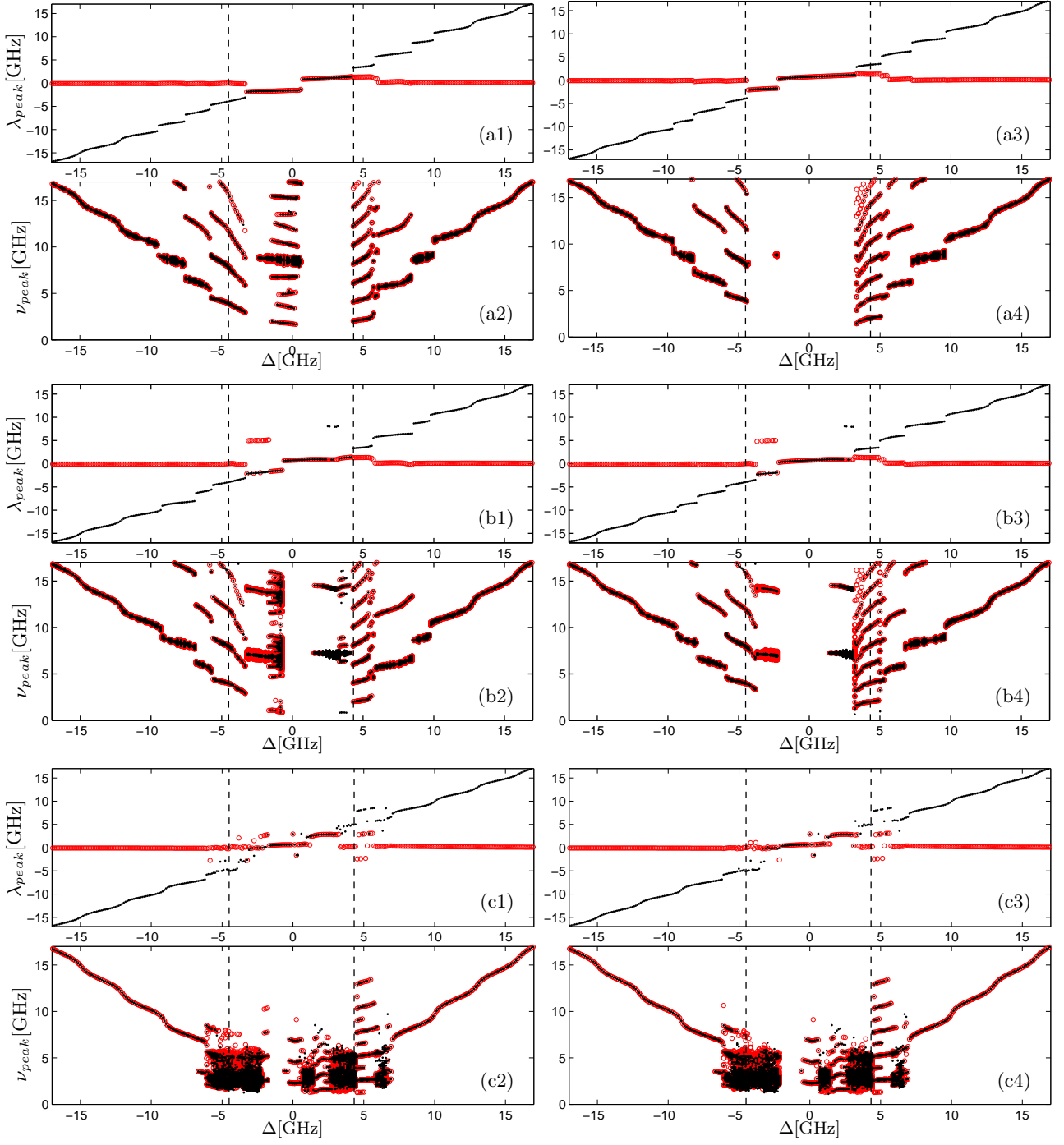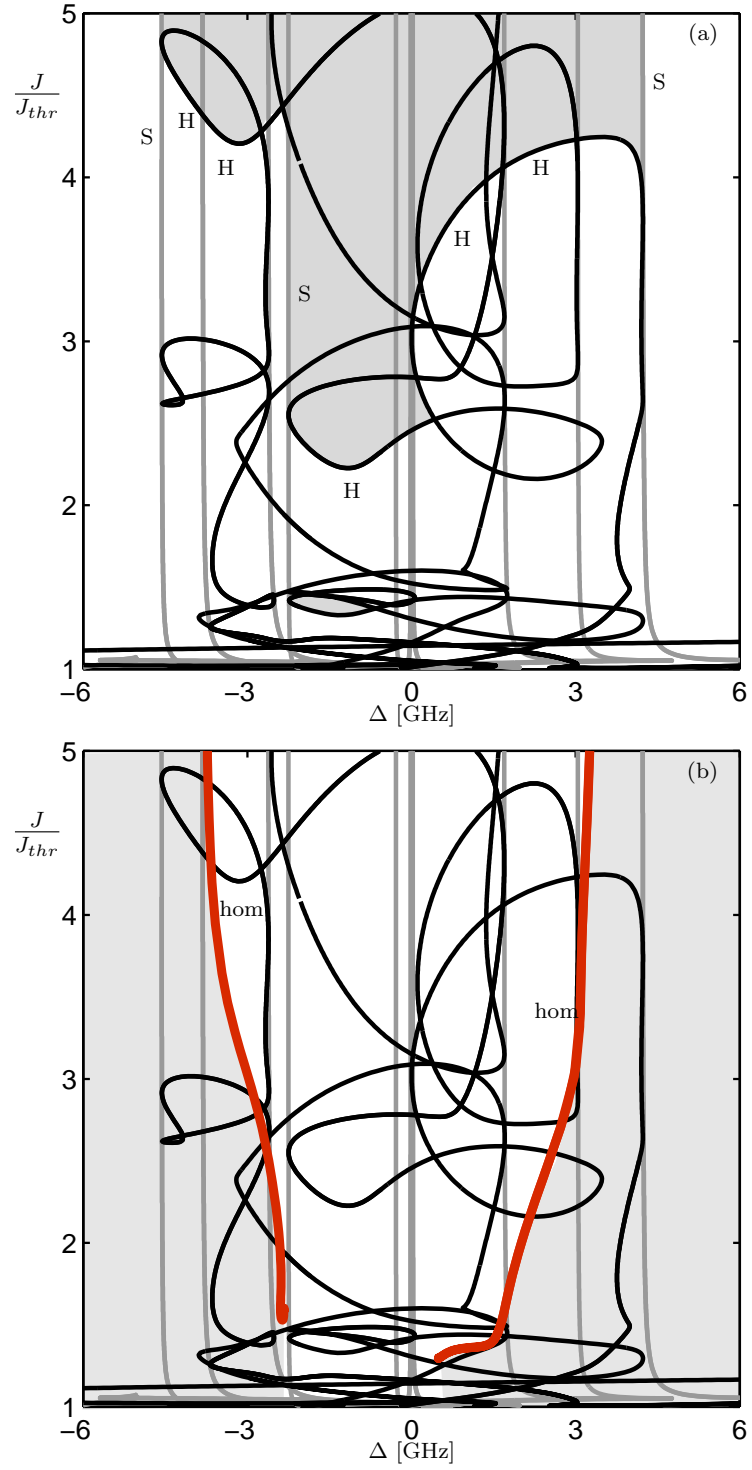
Figure 2. One-parameter bifurcation diagrams near the locking region for increasing (left column) and decreasing (right column) detuning Δ. Shown are the main peaks λ_{peak} in the optical spectrum and the main peaks ν_{peak} in the RIN-spectrum for laser 1 (red/gray) and laser 2 (black). Panels (a)–(c) are for a pump current of $J = 4.6 J_{thr}$, $J = 4 J_{thr}$ and $J = 1.38 J_{thr}$, respectively. The dotted vertical lines indicate the maximal width of the locking region (existence region of CLMs).

3

We now address the question when the delay-coupled semiconductor laser system is locked and what dynamics one encounters on the route into and out of locking. To this end, we characterize the different dynamics in terms of the optical spectra and the RIN-spectra (relative intensity noise) of both lasers. Figure 2 shows the dependence of the spectra on the detuning Δ as one-parameter bifurcation diagrams obtained by numerical integration of the governing rate equation model Eqns. (1)–(4). Specifically, main peaks in both the optical spectrum and the RIN-spectrum are plotted in black for laser 1 and in red/gray for laser 2. The dotted vertical lines indicate the maximal possible width of the locking region; inside this region CLMs exist (but they may either be stable or unstable), while outside this region there are no CLMs at all. Panels (a)–(c) are for three different values of the pump parameter J. To discover possible hysteresis loops we show in Figure 2 bifurcation diagrams for increasing (left column) and decreasing (right column) values of the detuning Δ.

Figure 2(a) shows the situation for a rather high pump current of $J = 4.6J_{thr}$ (in multiples of the threshold current J_{thr}), where panels (a1) and (a2) are for increasing detuning Δ and panels (a3) and (a4) for decreasing detuning. When the lasers are locked the optical frequency of both laser coincides. Locking can be observed in panels (a1) and (a3), but note the hysterisis effects at the boundary of the locking region. In addition to stable cw-emission undamped relaxation oscillations can be observed inside the locking region. Namely, the main peaks in the optical spectrum of both lasers still coincide, but the RIN-spectrum indicates intensity oscillations on the order of the relaxation oscillation frequency; see panels (a2) and (a4). For relaxation oscillations there is a pronounced hysteresis effect: there a large region of relaxation oscillations for increasing detuning [panel (a2)], whereas for decreasing detuning [panel (a4)] there are practically no relaxation oscillations. Note that the frequency of the relaxation oscillations is roughly constant, that is, it does not depend on Δ. Outside the locking region the dynamics of the coupled laser system is dominated by detuning oscillations. Specifically, from the optical spectra it can be seen that the main frequency of laser 2 is almost constant, whereas the frequency of laser 1 follows the detuning Δ with characteristic plateaus. The frequency distance between successive plateaux is proportional to the round-trip frequency of the gap between the two lasers; see Ref. [7] for details. From the RIN-spectra in Figure 2(a2) and (a4) it can be seen that the frequency of the detuning oscillation scales with the detuning Δ. Specifically, for $\Delta \to 0$ the frequency of the detuning oscillations goes to zero. This means that their period tends to infinity, which is indicative of a homoclinic bifurcation. Again hysteresis effects can be found at the boundaries of the locking region; namely, there is a region of bistability between detuning oscillations and stable cw-emission. Overall, for large values of the pump current J as in Figure 2(a) the dynamics is dominated by stable cw-emission, relaxation oscillations, and detuning oscillations, where higher harmonics in the spectra indicate a nonlinear profile of the oscillations.

For lower pump currents the dynamics of the coupled laser system becomes more complicated, in particular, around zero-detuning. Figure 2(b) illustrates this with bifurcation diagrams for $J = 4J_{thr}$. Concentrating on panels (b1) and (b2) for increasing detuning, we again find detuning oscillation for large negative Δ. As the detuning is increased, higher harmonics of the detuning oscillation frequency can be found in the RIN-spectrum. Eventually, around $\Delta \approx -4$ GHz the detuning oscillations disappear and relaxation oscillations are observed. The broadening of the relaxation oscillation peaks indicates additional bifurcations and more complicated dynamics. Around zero detuning there is an interval of stable cw-emission, which become unstable in a Hopf bifurcation around $\Delta = 2$ GHz where they give rise to more relaxation oscillations. At around $\Delta = 4.2$ GHz these relaxation oscillations disappear and detuning oscillations are observed. Hysteresis effects can again be observed by comparing panels (b1), (b2) for increasing detuning with panels (b3), (b4) for decreasing detuning. For even lower pump currents, as illustrated in Figure 2(c) for $J = 1.38J_{thr}$, more complicated or even chaotic dynamics can be found. There is now only a small detuning interval around $\Delta = -1$ GHz, where the coupled laser system shows stable cw-emission. On the other hand, for very large detuning the dynamics is again dominated by detuning oscillations. For this low value of the pump current almost no hysteresis is found, that is, there is no bistability of different dynamical attractors; compare Figure 2(c2) and (c4).

Overall, the dynamics of the coupled semiconductor laser system exhibits three characteristic time scales: the detuning frequency, the relaxation oscillation frequency, and the round-trip frequency of the light (associated with the time delay τ). Relaxation oscillations are found for rather small values of detuning in the range $\Delta = [-4.6; 4.2]$ GHz, when CLMs bifurcate in Hopf bifurcations. By contrast, detuning oscillations are found mainly outside the maximal locking region, that is, for quite large values of Δ. The round-trip frequency is observed as characteristic jumps in the optical frequency of the lasers.

4

Figure 3. Two-parameter bifurcation diagrams in the (Δ, J)-plane of detuning versus pump current. Shown are curves of saddle-node bifurcations (S), Hopf bifurcations (H), and homoclinic bifurcations (hom); in panel (a) the gray shading indicates the region stable CLMs and in panel (b) it indicates the region of stable dynamics associated with detuning oscillations.

3. TWO-PARAMETER BIFURCATION ANALYSIS

To get more insight into the dependence of the route to locking on the pump parameter J, we now present a two-parameter bifurcation diagram in the (Δ, J)-plane. To this end, we perform a bifurcation study of the rate equation model Eqns. (1)–(4) with the numerical continuation packages DDE-BIFTOOL [15] and PDDE-CONT [16]. In this way, we find and follow bifurcation curves in the (Δ, J)-plane that correspond to qualitative transitions in the dynamics of the delay-coupled semiconductor laser system. This provides a more global view of the stability regions of the different dynamics, including stable cw-emission, relaxation oscillations and detuning oscillations.

Figure 3 shows two bifurcation diagram in the (Δ, J)-plane, where we concentrate on the locking region around zero detuning and the instabilities at the boundary of the locking region. Panel (a) concentrates on the stability region of the CLMs, that is, on the parameter region where one finds stable locking of the delay-coupled laser system. The CLMs appear and disappear in pairs in saddle-node (S) bifurcations. The two outermost saddle-node bifurcations, at around $\Delta = -4.6$ GHz and $\Delta = +4.2$ GHz, mark the maximum possible width of the locking region; in Figure 2 this was indicated by the dotted lines. Outside this detuning interval there are no CLMs. Note that there are additional saddle-node bifurcation (closer to zero detuning) that give rise to additional CLMs, some of which may be stable. Importantly, the outermost saddle-node bifurcation curves bound the region of stable CLMs only for quite large value of the pump current, namely for $J > 4.8 J_{thr}$ on the left and $J > 3.9 J_{thr}$ on the right, respectively. For lower values of the pump current the CLMs lose their stability in Hopf (H) bifurcations, which give rise to the relaxation oscillations that were observed in Figure 2. Note that for $J < 2.2 J_{thr}$ one typically does not find any stable CLMs, that is, the two delay-coupled lasers only lock reliably when the pump current is sufficiently above threshold.

Figure 3(b) concentrates on the detuning oscillations, which dominate the dynamics outside the locking region. As was observed in the previous section, the period of the detuning oscillations tends to infinity as the detuning is decreased towards zero. Panel (b) shows that this fact is indeed due to homoclinic bifurcations: the two disjoint gray regions of stable dynamics associated with detuning oscillations are bounded by two curves of homoclinic bifurcations, one at negative Δ and one at positive Δ. It should be noted that not all detuning oscillations that bifurcate from these two homoclinic bifurcation curves are stable. Specifically, for pump currents below $J \approx 3.0 J_{thr}$ detuning oscillations are initially unstable. Nevertheless, the dynamics near the curves of homoclinic bifurcation is associated with the detuning oscillations, meaning that it strongly features their frequency components. As the magnitude $|\Delta|$ increases, the unstable detuning oscillations undergo a complicated sequence of bifurcations (including saddle-node of limit cycle bifurcations, period-doubling bifurcations, and torus bifurcations), that eventually leads to stable detuning oscillations. For rather high pump currents the bifurcation structure is less complicated and the detuning oscillations become stable soon after they are born in the homoclinic bifurcation. This is in agreement with the numerical observations in Figure 2.

4. CONCLUSIONS

We have studied the dynamics near the locking region of two mutually delay-coupled semiconductor lasers by means of a bifurcation analysis of a rate equation model for the optical fields and the inversions of the lasers. In this way, we characterized the different dynamics of the coupled laser system and found stable cw-emission, relaxation oscillations, detuning oscillations and complicated, possibly chaotic dynamics. Two bifurcation diagrams in the plane of detuning versus the pump current provided a global view of the underlying bifurcation structure of this delay-coupled laser system. A comparison with experimental measurements by I. Fischer and E. Wille will be presented elsewhere. The dependence of the dynamics and bifurcations near the locking region on other parameters, such as the feedback phase or the linewidth enhancement factor, is an interesting topic for further research.

ACKNOWLEDGMENTS

REFERENCES

1. G. D. VanWiggeren and R. Roy, "Communication with chaotic lasers," *Science* **279**, pp. 1198–1200, 1998.

2. M. T. Hill, , H. J. S. Dorren, T. de Vries, X. J. M. Leijtens, J. H. den Besten, B. Smalbrugge, Y. Oei, H. Binsma, G. Khoe, and M. K. Smit, "A fast low-power optical memory based on coupled micro-ring lasers," *Nature* **432**, pp. 206–209, 2004.

3. M. Möhrle, B. Sartorius, C. Bornholdt, S. Bauer, O. Brox, A. Sigmund, R. Steingrüber, M. Radziunas, and H.-J. Wünsche, "Detuned grating multisection-RW-DFB lasers for high speed optical signal processing," *IEEE J. Select. Topics Quantum Electron.* **7**, pp. 217–223, 2001.

4. H. Schuster and P. Wagner, "Mutual entrainment of two limit cycle oscillators with time delayed coupling," *Progr. Theor. Phys.* **81**, pp. 939–945, 1989.

5. I. Fischer, Y. Liu, and P. Davis, "Synchronization of chaotic semiconductor laser dynamics on subnanosecond time scales and its potential for chaos communication," *Phys. Rev. A* **62**, p. 011801, 2000.

6. T. Heil, I. Fischer, W. Elsäßer, J. Mulet, and C. R. Mirasso, "Chaos synchronization and spontaneous symmetry-breaking in symmetrically delay-coupled semiconductor lasers," *Phys. Rev. Lett.* **86**, pp. 795–798, 2001.

7. H.-J. Wünsche, S. Bauer, J. Kreissl, O. Ushakov, N. Korneyev, F. Henneberger, E. Wille, H. Erzgräber, M. Peil, W. Elsäßer, and I. Fischer, "Synchronization of delay-coupled oscillators: A study on semiconductor lasers," *Phys. Rev. Lett.* **94**, p. 163901, 2005.

8. M. Peil, T. Heil, I. Fischer, and W. Elsäßer, "Synchronization of chaotic semiconductor laser systems: A vectorial coupling-dependent scenario," *Phys. Rev. Lett.* **88**, p. 174101, 2002.

9. J. Mulet, C. Mirasso, T. Heil, and I. Fischer, "Synchronization scenario of two distant mutually coupled semiconductor lasers," *J. Opt. B: Quantum Semiclass. Opt.* **6**, pp. 97–105, 2004.

10. E. Wille, M. Peil, I. Fischer, and Elsäßer, "Dynamical scenarios of mutually delay-coupled semiconductor lasers in the short coupling regime," *in: Semiconductor Lasers and Laser Dynamics, Proceedings of SPIE (D. Lenstra, G. Morthier, T. Erneux, and M. Pessa; Eds.)* **5452-05**, pp. 41–50, 2004.

11. C. M. González, C. Masoller, M. C. Torrent, and J. García-Ojalvo, "Synchronization via clustering in a small delay-coupled laser network," *EPL (Europhysics Letters)* **79**(6), p. 64003 (6pp), 2007.

12. H. Erzgräber, B. Krauskopf, and D. Lenstra, "Coupled laser modes of mutually delay-coupled lasers," *SIAM J. Appl. Dyn. Syst.* **5**(1), pp. 30–65, 2006.

13. R. Lang and K. Kobayashi, "External optical feedback effects on semiconductor injection laser properties," *IEEE J. Quantum Electron.* **QE-16**, pp. 347–355, 1980.

14. J. Mulet, C. Masoller, and C. R. Mirasso, "Modeling bidirectionally coupled single-mode semiconductor lasers," *Phys. Rev. A* **65**, p. 063815, Jun 2002.

15. K. Engelborghs, T. Luzyanina, and G. Samaey, "DDE-BIFTOOL v. 2.00 user manual: a matlab package for bifurcation analysis of delay differential equations.," Technical Report TW-330, Department of Computer Science, K. U. Leuven, Leuven, Oct. 2001.

16. R. Szalai, "PDDE-CONT: A continuation and bifurcation software for delay-differential equations," technical report, Department of Applied Mechanics, Budapest University of Technology and Economics, 2005.